FERMILAB-TM-2210
TESLA-FEL 2003-01, May 2003

Higher Order Modes of a 3rd Harmonic Cavity with an Increased End-cup Iris

T. Khabibouline [1]), N. Solyak [1]), R.Wanzenberg [2])
[1]) FERMILAB, P.O. Box 500, Illinois 60510, USA
[2]) DESY, Notkestr. 85, 22603 Hamburg, Germany

Abstract

The cavity design for a 3rd harmonic cavity for the TTF 2 photoinjector has been revised to increase the coupling between the main coupler and the cavity cells. The iris radius of the end cup of the cavity has been increased to accomplish a better coupling. The basic rf-parameters and the higher order modes of the modified design are summarized in this report.

Introduction

For the phase 2 of the TESLA test facility (TTF 2) it has been planed to use a cavity operated at three times the 1.3 GHz frequency of the existing TTF 1 cavities to compensate nonlinear distortions of the longitudinal phase space [1]. A cavity design for a 3.9 GHz pi-mode cavity by J. Sekutowicz has been discussed in [2] with respect to the basic rf-parameters and the higher order mode (HOM) properties. The design of the end cups has been recently revised to improve the coupling from the main coupler to the cavity cells. The cavity geometry and the energy density of the electric field of the accelerating mode calculated with HFFS [3] is shown in Figure 1.

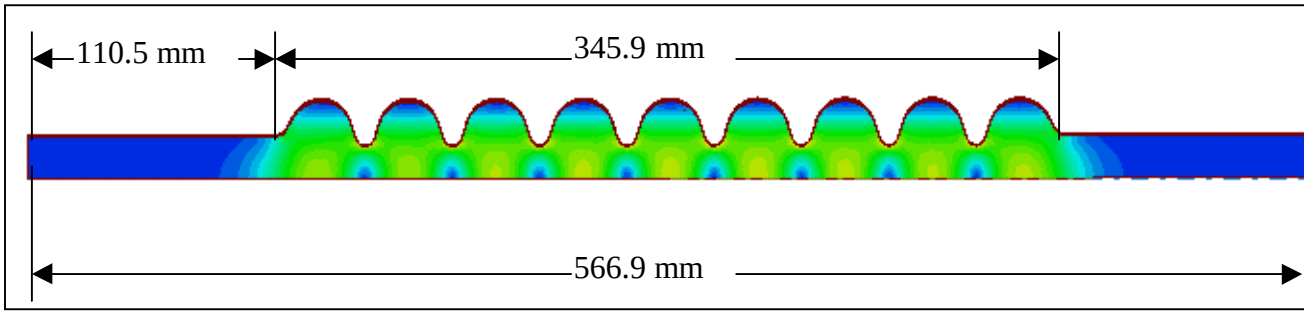

Figure 1: Geometry of the third harmonic cavity with an increased end-cup iris

A sketch of the cell geometry is given in Figure 2. The parameters of the mid-cell and the end-cell are listed in Table 1. The mid-cup and end-cup#0 geometry corresponds to the cavity design which is discussed in the report [2]. The new end-cup parameters are listed in the last column of the table labeled as end-cup#1. The iris radius has been increased to 20 mm. This is just the radius of the beam pipe. A cavity based on the mid-cup und end-cup#1 geometry will be discussed throughout this report.

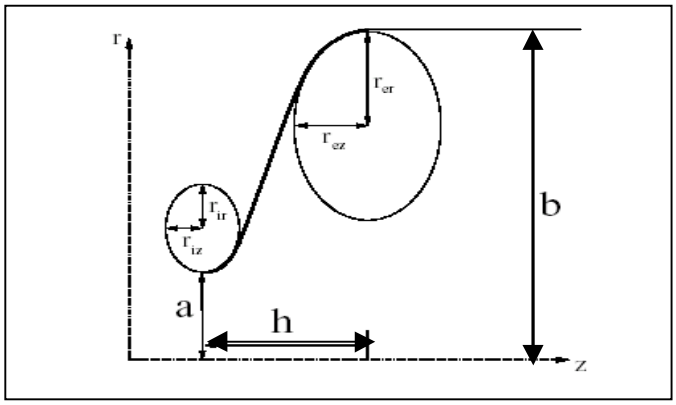

Figure 2: Sketch of the cell geometry.

		mid-cup	end-cup#0 (DESY)	end-cup#1 (Fermilab)
Iris radius, *a*	mm	15.0	15.0	20.0
Equator radius, *b*	mm	35.787	35.787	35.787
Half cell length, *h*	mm	19.2167	19.2167	19.2167
Curvature at:				
Equator – horiz. axis, r_{ez}	mm	13.6	12.0813	14.4
- Vert. axis, r_{er}	mm	15.0	15.0	15.0
Iris – horiz. Axis, r_{iz}	mm	4.5	4.5	4.5
- Vert axis, r_{ir}	mm	6.0	6.0	6.0

Table 1: Parameter of the cup geometry.

In these report we will present the basic rf parameters like frequency, R/Q-value, Q-value and G_1 for many monopole, dipole and quadrupole modes. The following convention has been adopted for the characteristic rf parameter R/Q and G_1:

$$\frac{R}{Q} = \frac{|V_z(r)|^2}{4\pi\, f\, U}\,, \qquad G_1 = R_{sur}\; Q_0\;,$$

where f is the frequency of the mode, U is the total stored energy in the mode, $V_z(r)$ is the voltage at the radial position r, R_{sur} is the surface resistence and Q_0 is the quality factor or unloaded Q-value of the mode. The Q-value is calculated from the stored energy U and the power P_{sur} dissipated into the cavity wall: $Q_0 = 2\pi\; f\; U / P_{sur}$. The voltage is calculated from the electric field according to: $V_z(r) = \int dz\; E_z(r,z)\; \exp(-i\;\; 2\pi\; f\;\; z/c)$.

The passband structure of the mid-cell

The monopole, dipole and quadrupole passbands of the cavity midcell have been studied using the MAFIA [4] eigenvalue solver. Periodic boundary conditions have been applied across one cavity mid-cell:

$$\vec{E}(r, z+g) = \vec{E}(r, z+g)\ \exp(i\ \phi)$$

where ϕ is the phase advance per cell, and g the cell length. The phase advance per cell is used as an abscissa in the plot of the passbands in Figure 4, Figure 5 and Figure 6. A beam excites most strongly those modes which are synchronous to the beam, i.e. modes with a phase velocity equal to the speed of light, or which are close to the light cone. The light cone is the straight line

$$f(\phi) = \frac{c}{2\pi}\ \frac{\phi}{g},$$

which is folded into the phase range from 0 to 180 degree using the periodicity of the structure.
The gap length of a cavity cell is chosen such that the 3.9 GHz pi-mode is synchronous to the beam. The electric field distribution in a mid-cell is shown in Figure 3.

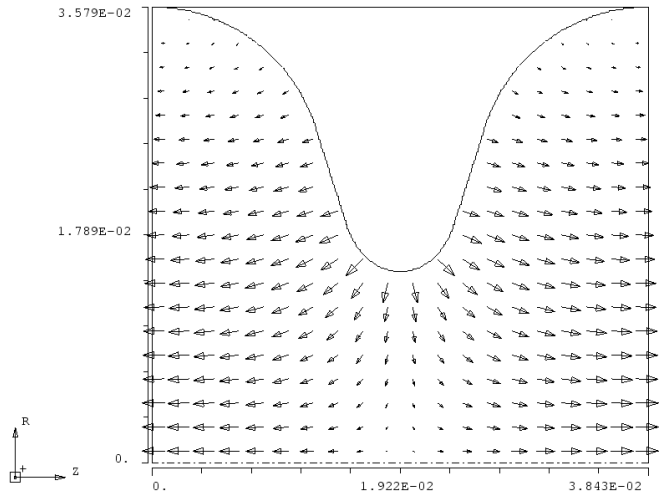

Figure 3: Electric field of the accelerating pi-mode in a mid-cell of the 3.9 GHz cavity calculated with the MAFIA eigenvalue solver.

Eight monopole passbands have been calculated for the mid-cell geometry. The lowest passbands contains the accelerating mode with a frequency close to 3.9 GHz. All monopole passbands below a frequency of 14 GHz are shown in Figure 4. The highest impedances values are found for the modes where the light cone crosses the passbands. That is by design the 3.9 GHz accelerating mode and higher order monopole modes above 7 GHz as shown in Figure 4.

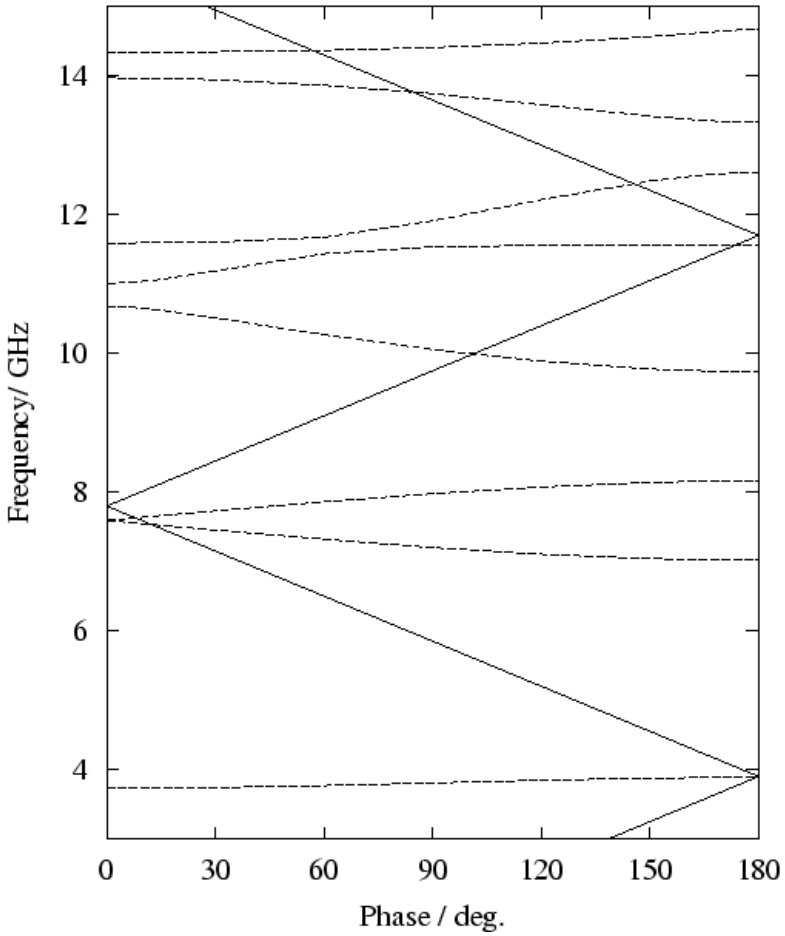

Figure 4: Monopole passbands of a cavity mid-cell.

The long range wakes due to higher order dipole modes can cause kicks on the bunches, which can result in orbit deviations within the bunch trains or even an cumulative beam-breakup instability. Therefore it is important to know the R/Q-value and the Q value of the dipole modes. The detailed mode structure of a 9-cell cavity is discussed in a later section of the report. The passband structure of a single mid-cell give already first information which dipole modes are mostly excited by the beam. The dipole passbands up-to a frequency of 10 GHz are shown in Figure 5. There are six passband in that frequency range. If a bunch transverses the cavity with a large offset, say more than 1 cm, the contribution of quadrupole modes to the long range wakefield is important. Therefore the lowest quadrupole passbands have also been calculated. The passbands up-to a frequency of 11 GHz are shown in Figure 6.

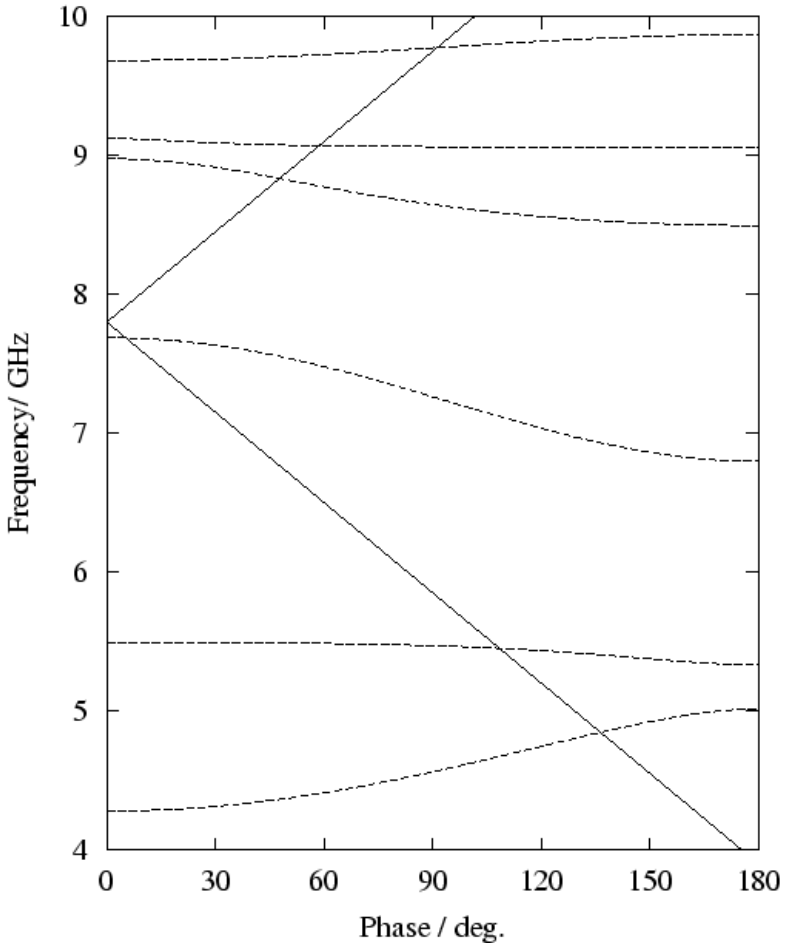

Figure 5: Dipole passbands of the cavity midcell.

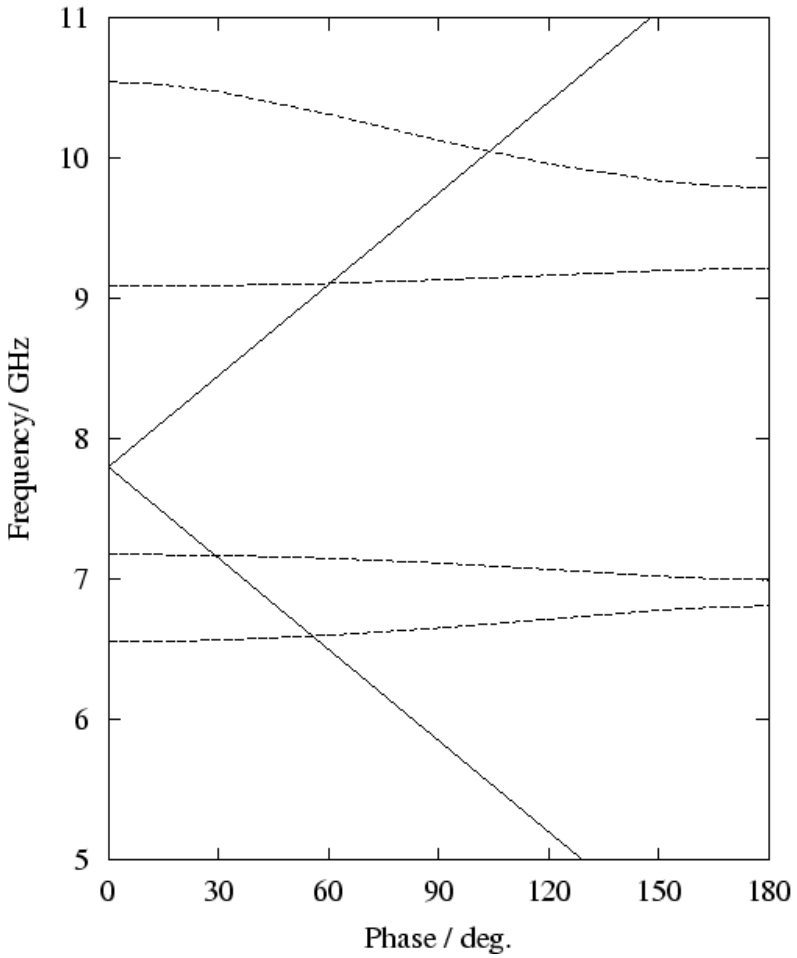

Figure 6: Quadrupole passbands of the cavity midcell.

The accelerating mode and higher order monopole modes

In this section we present the result for the monopole modes of a 9-cell cavity. The basic design parameters of the accelerating mode are given in Table 1. The electric field of the accelerating mode is shown in Figure 7 (MAFIA calculation) and previously in Figure 3 (HFFS calculation).

3rd harmonic cavity with increased end cell iris diameter		
design parameter:		
Type of accelerating structure	standing wave	
Accelerating mode	pi-mode	
Frequency	3.9	GHz
Active Length	345.9	mm
Number of cells	9	
R/Q	375	Ohm
Geometry factor (G1)	262	Ohm
Nominal accelerating gradient	20	MV/m
Stored energy (20 MV/m)	2.6	J
Epeak/Eacc	2.5	
Bpeak (20 MV/m)	0.11	T

Table 2: Accelerating mode parameters of the 3rd harmonic cavity with increased end cell iris diameter.

Figure 7: Electric field of the accelerating pi-mode (MAFIA calculation).

For the MAFIA calculation, electric boundary conditions equivalent to a electric shorting plate have been used at both ends of the cavity. The boundary conditions are important for all modes above the cut-off frequency of the beam pipe. The first 40 monopole modes of the 9-cell cavity have been calculated with the MAFIA code. The R/Q of these modes are shown in Figure 8 using a linear scale and in Figure 9 using a logarithmic scale. A complete listing of the rf-parameters is given in Appendix A. The modes with the largest R/Q from these list are the accelerating mode (# 9) and mode #26 with a frequency of 7.5765 GHz. The electric field of the mode # 26 is shown in Figure 10. The mode # 26 has large electric field components in the beam pipe. Therefore it should be easy to damp this mode with HOM couplers. A large R/Q is expected for this mode from the passband structure of one cavity mid-cell, since the light cone crosses the 2nd and 3rd monopole passbands close to the frequency of mode #26 (see Figure 4). Only the modes of the first passband are below the cutoff frequency of the beam pipe, which is 5.7372 GHz for TM monopole modes.

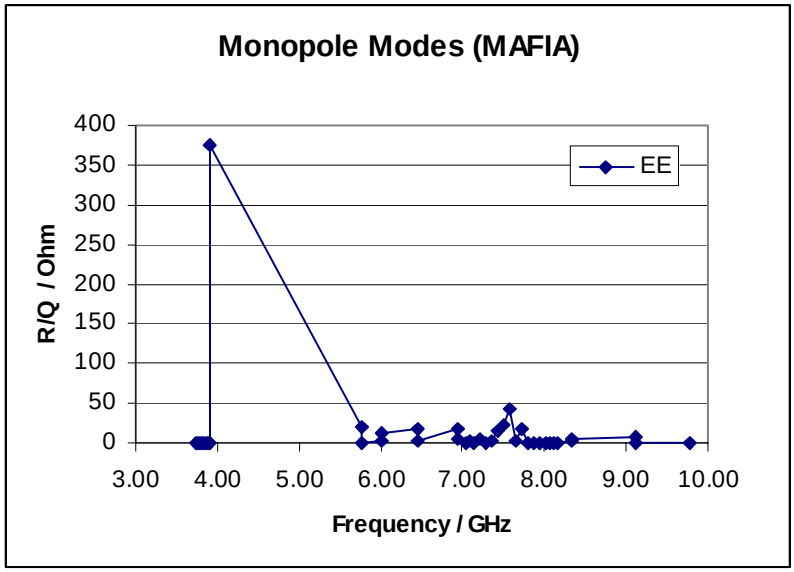

Figure 8: R/Q of monopole modes in a 9-cell cavity versus frequency (MAFIA results).

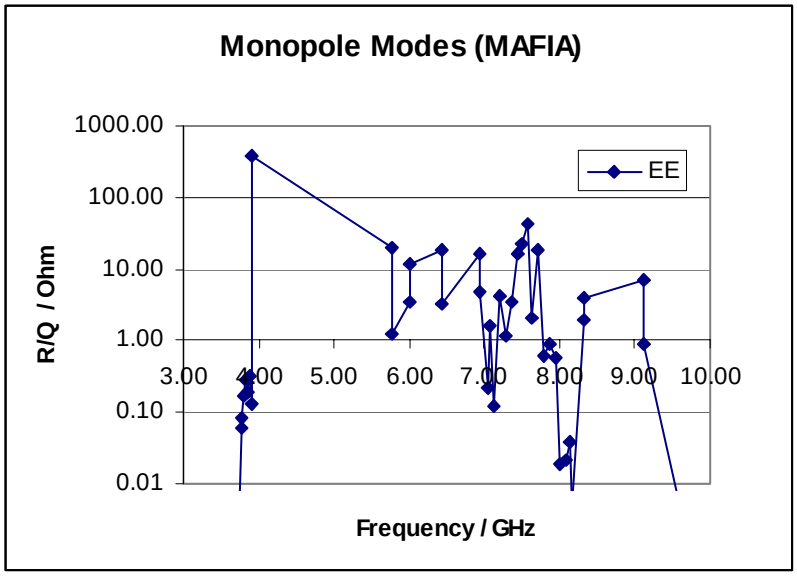

Figure 9: Logarithmic presentation of R/Q of monopole modes in a 9-cell cavity versus frequency.

Figure 10: Electric field of the higher monopole mode #26, f = 7.5765 GHz.

Dipole Modes

To calculate the kicks on bunches in a bunch train it is important to know the long range wakes due to higher order dipole modes. The kick on the bunch j due to the wake field is:

$$\vec{\theta}_j = \frac{eq}{E_j} \sum_{i<j} (x_i \vec{e}_x + y_i \vec{e}_y)\ W_\perp^{(1)}(s_j - s_i).$$ e is the charge of one electron, q the charge in one bunch, E_j the energy of bunch j, $\vec{e}_x, \vec{e}_y$ are unit vectors in the transverse direction, x_i, y_i are the transverse offsets of bunches previous to bunch j and s_i is the longitudinal position of the bunches i. The transverse dipole mode wake potential $W_\perp^{(1)}(s)$ can be written as a sum over all dipole modes:

$$W_\perp^{(1)}(s) = c \sum_n \left(\frac{R^{(1)}}{Q}\right)_n \sin(2\pi\ f_n s/c)\ \ \exp(-\frac{2\pi\ f_n}{2Q_n} s/c).$$

f_n is the frequency, $(R^{(1)}/Q)_n$ is the dipole mode R/Q-value, Q_n the total Q-value of mode n and c is the velocity of light. The Q-value is usually dominated by the external Q due to higher order mode couplers. The dipole mode $(R^{(1)}/Q)_n$ value is obtained from an R/Q at the radial position r as: $\frac{R^{(1)}}{Q} = \frac{1}{r^2}\left(\frac{R}{Q}\right)(r)$.

The computer codes HFFS [3] and MAFIA [4] have been used to calculate R/Q values of all dipole modes up to a frequency of about 10 GHz. Electric (EE) and magnetic (MM) boundary conditions are applied at both ends of the cavity. The R/Q –value of most of the modes depend on the boundary conditions since almost all modes can propagate in the beam pipe. The cutoff frequency of the beam pipe is 4.392 GHz for TE dipole modes. The electric field of the dipole mode with the lowest frequency of 4.15 GHz in the cavity is shown in Figure 11.

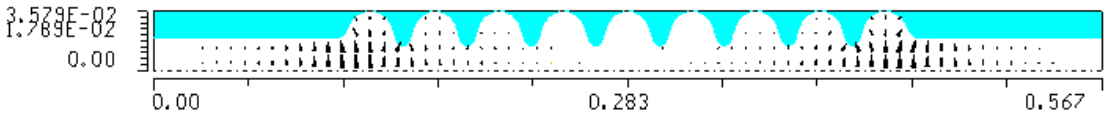

Figure 11: Electric field of the dipole mode #1, f=4.15 GHz (EE boundary condition, MAFIA calculation).

The electric field of this mode already leaks out of the cavity into the beam pipe. The dipole mode with the highest R/Q value (about 50 Ohm/cm^2) is show in Figure 12 and Figure 13. The results for all dipole modes calculated with MAFIA are shown in Figure 14 and the results calculated with HFFS are shown in Figure 15.

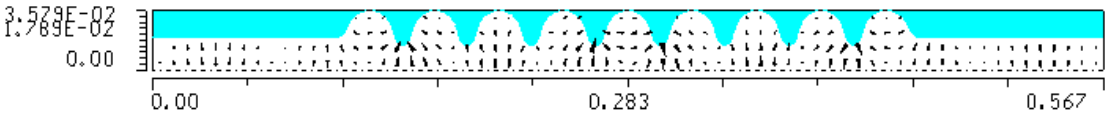

Figure 12: Electric field of the dipole mode #10, f=4.83 GHz, R/Q = 50.7 Ohm/cm^2 (EE boundary condition, MAFIA calculation).

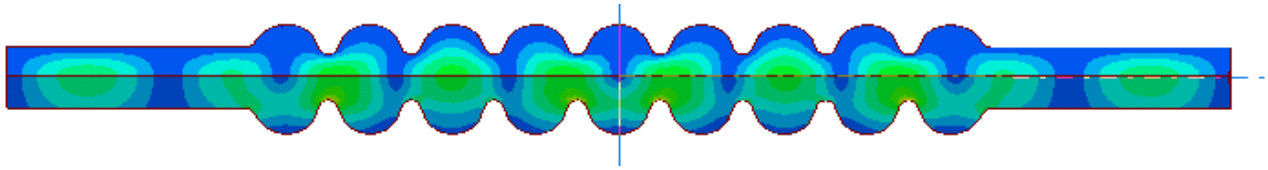

Figure 13: Electric field distribution of the dipole mode #10, f=4.82 GHz, R/Q = 49.85 Ohm/cm^2 (HFFS calculation, quarter of cavity: top side - M boundary, bottom - E boundary, ends - E boundary).

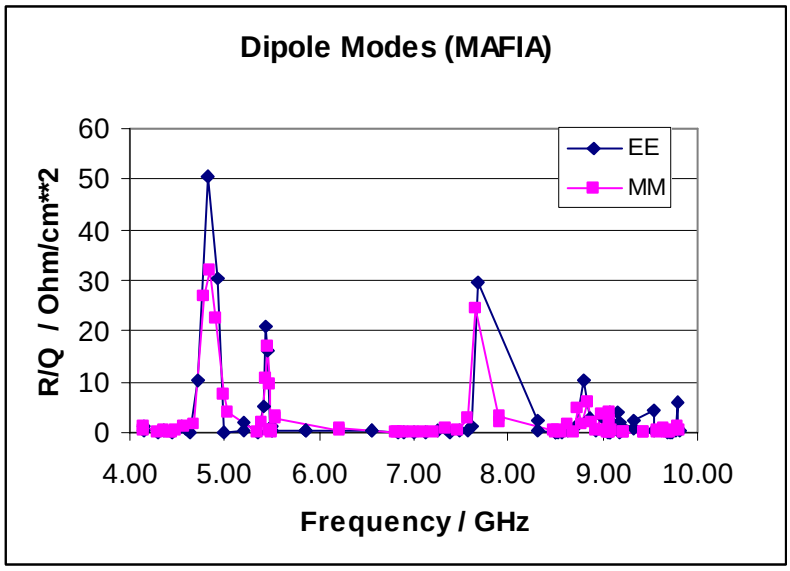

Figure 14: R/Q values of dipole modes (EE and MM boundary conditions, MAFIA calculation)

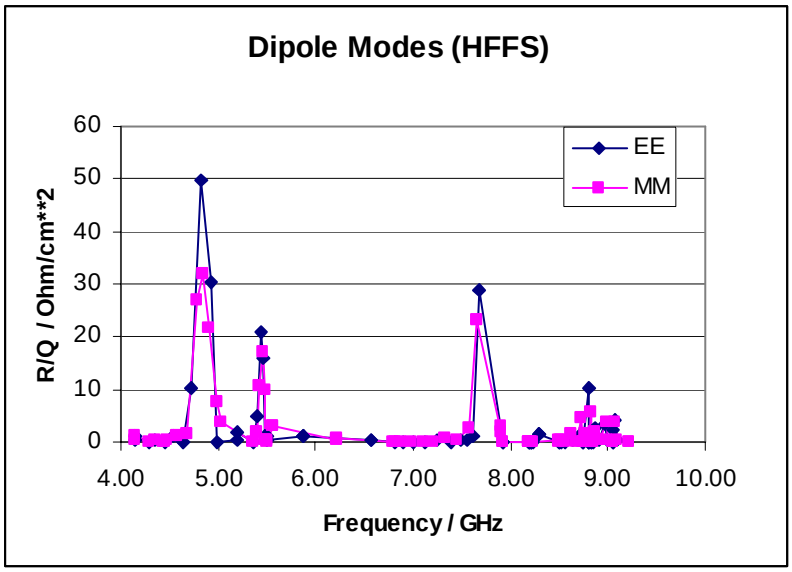

Figure 15: R/Q values of dipole modes (EE and MM boundary conditions, HFFS calculation)

A complete listing of the data shown in Figure 14 and in Figure 15 can be found in the Appendix B. The data from both codes MAFIA and HFFS agree very well with respect of the R/Q value. All data are shown in Figure 16 using a logarithmic scale for the R/Q axis.

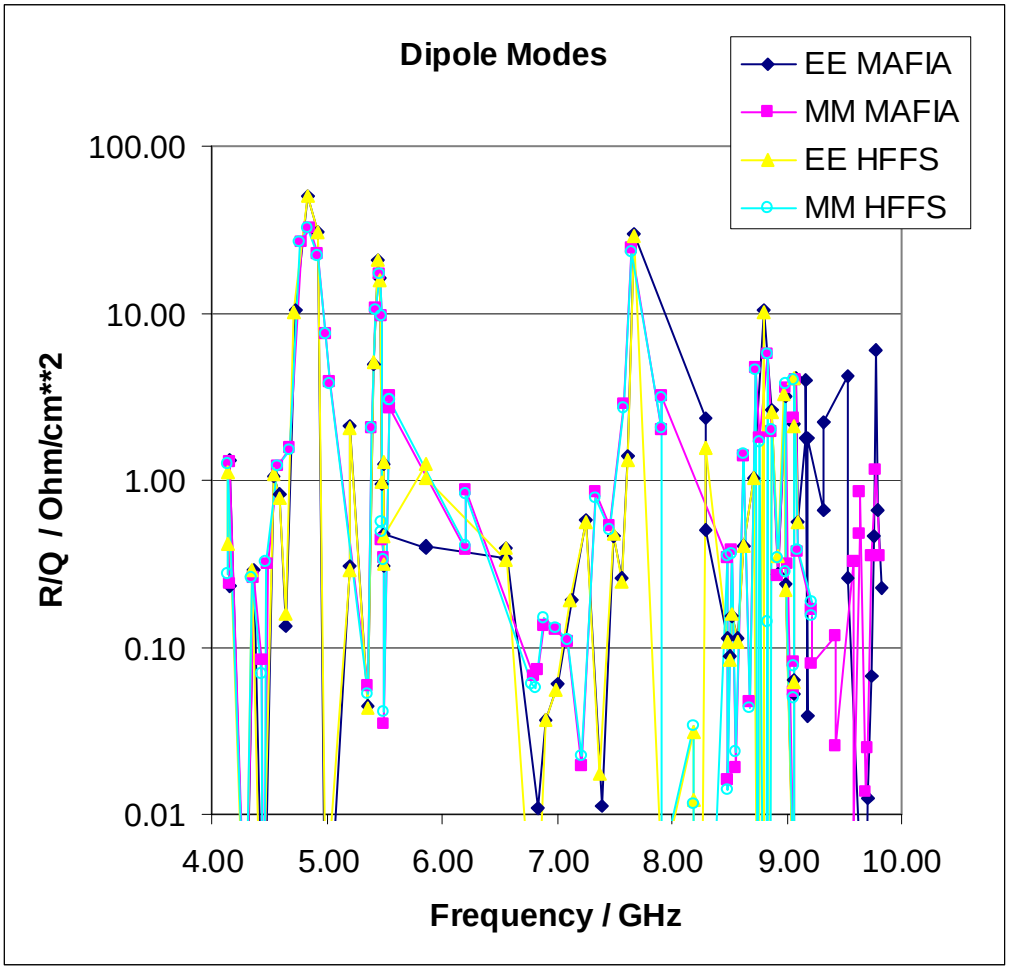

Figure 16: Comparison of the R/Q values obtained with MAFIA and HFFS.

Further electric field distributions of modes with a high value for R/Q are shown in Figure 17, Figure 18, Figure 19, Figure 20 and Figure 21. We have picked from each peak in the R/Q plot (see Figure 16) one example to show the details of the electric fields. The mode numbers corresponds to the list of modes from the Appendix B found with MAFIA and HFFS. The HFFS code has found more modes with frequencies above 8 GHz than the MAFIA eigenvalue solver. The number of the mode differs therefore between the HFFS and MAFIA calculations.
The electric field in the beam pipe of the mode #36 (MAFIA and HFFS number) is by a factor of about 4 smaller than the electric field in center cell of the cavity.

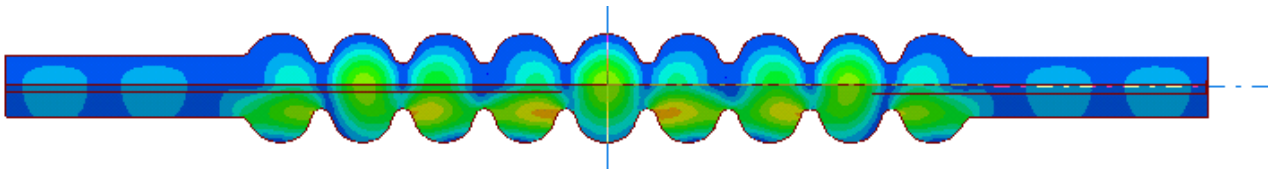

Figure 17: Electric field distribution of the dipole mode #17, f=5.44 GHz, R/Q = 20.9 Ohm/cm^2 (HFFS calculation, quarter of cavity: top side - M boundary, bottom - E boundary, ends - E boundary).

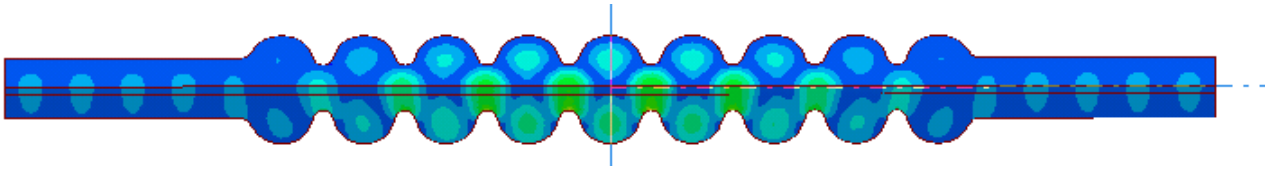

Figure 18: Electric field distribution of the dipole mode #36, f=7.66 GHz, R/Q = 28.9 Ohm/cm^2 (HFFS calculation, quarter of cavity: top side - M boundary, bottom - E boundary, ends - E boundary).

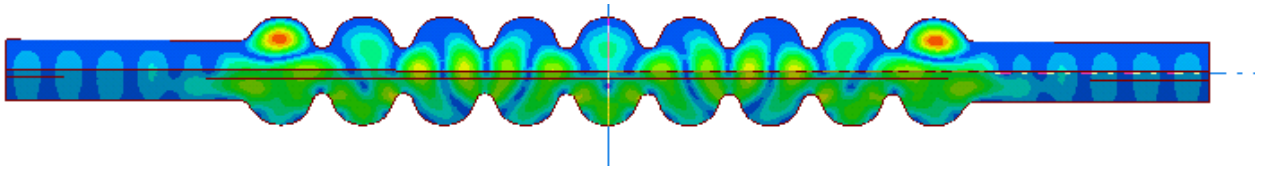

Figure 19: Electric field distribution of the dipole mode #56, f=8.79 GHz, R/Q = 10.22 Ohm/cm^2 (HFFS calculation, quarter of cavity: top side - M boundary, bottom - E boundary, ends - E boundary).

The mode #69 (HFFS number) or #53 (MAFIA number), which is shown in Figure 20 and Figure 21, has almost no electric field in the beam pipe and even the cavity end cells. The radial electric field component as a function of the longitudinal position z is shown in Figure 22. The field in beam pipe is by a factor of about 25 smaller than the field inside the cavity. This indicates that it could be difficult to damp this mode with HOM-couplers.

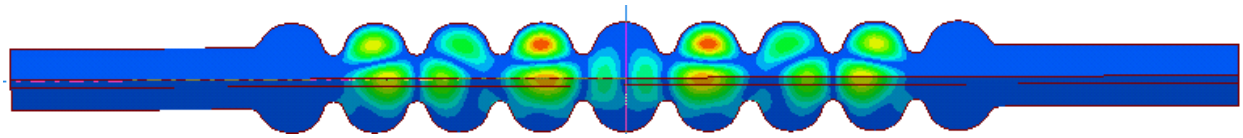

Figure 20: Electric field distribution of the dipole mode #69, f=9.05 GHz, R/Q = 2.1 Ohm/cm^2 (HFFS calculation, quarter of cavity: top side - M boundary, bottom - E boundary, ends - E boundary).

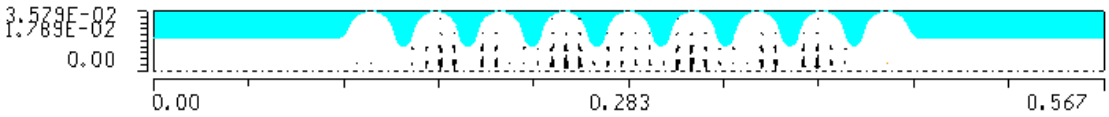

Figure 21: Electric field of the dipole mode #53, f=9.06 GHz, R/Q = 2.2 Ohm/cm^2 (EE boundary condition, MAFIA calculation).

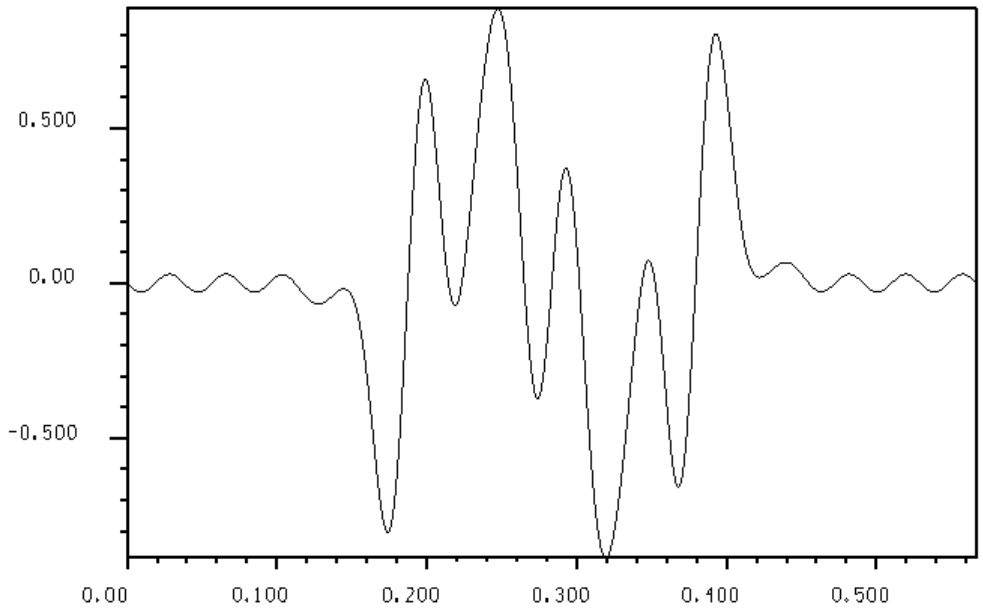

Figure 22: Radial field component of the electric field versus z of the dipole mode #53, f=9.06 GHz, (EE boundary condition, MAFIA calculation). The field component E_r (r,z) is plotted at the radial position r= 1 cm.

Quadrupole Modes

A second order contribution to the transverse long range wake potential is due to quadrupole modes in the cavity. The total transverse wake due to bunch # i on the trailing bunch # j in a bunch train may be written in term of the dipole and quadrupole wake potential as:

$$\vec{W}_\perp(x_j, y_j, x_i, y_i, s_j - s_i) \approx (x_i\vec{e}_x + y_i\vec{e}_y)\ W_\perp^{(1)}(s_j - s_i) + (x_j\vec{e}_x - y_j\vec{e}_y)\ 2\,(x_i^{\,2} - x_i^{\,2})\ W_\perp^{(2)}(s_j - s_i) + (x_j\vec{e}_x + y_j\vec{e}_y)\ 2\,(2x_i y_i)\ W_\perp^{(2)}(s_j - s_i)$$

The quadrupole and skew quadrupole components of the transverse wake potential depend on the transverse positions x_i, y_i of the bunch which generate the wake *and* on the transverse positions x_j, y_j of the trailing bunch. The quadrupole wake potential $W_\perp^{(2)}(s)$ can be written as a sum of all quadrupole modes like for the dipole modes but using the quadrupole R/Q-value $(R^{(2)}/Q)_n$, which is obtained from an R/Q at the radial position r as:

$$\frac{R^{(2)}}{Q} = \frac{1}{r^4}\left(\frac{R}{Q}\right)(r).$$

The best way to compare the R/Q values of dipole modes and Quadrupole modes is to plot R/Q for a fixed beam offset in the cavity. The R/Q value of the quadrupole modes are show in Figure 23 and listed in the appendix C. A comparison of the R/Q-values of the dipole and quadrupole modes (EE boundary condition) is shown in Figure 24.

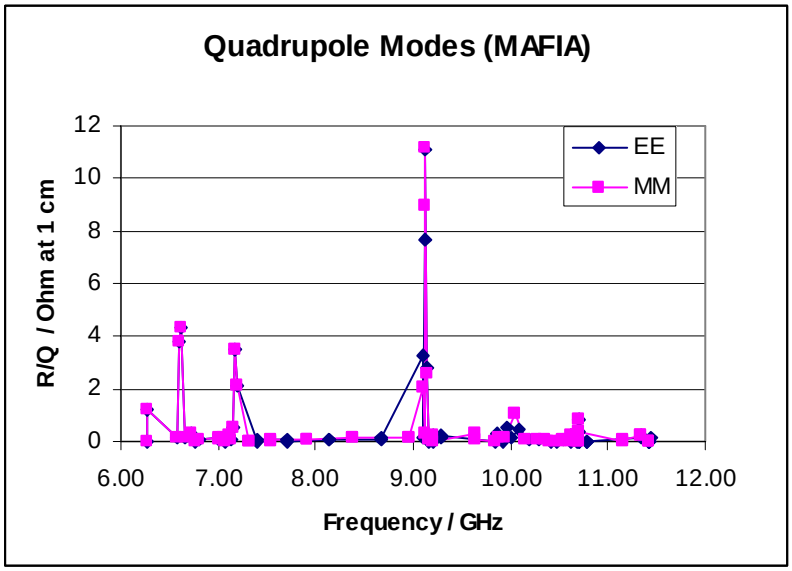

Figure 23: R/Q values of quadrupole modes (EE and MM boundary conditions, MAFIA calculation) at an radial offset of 1 cm.

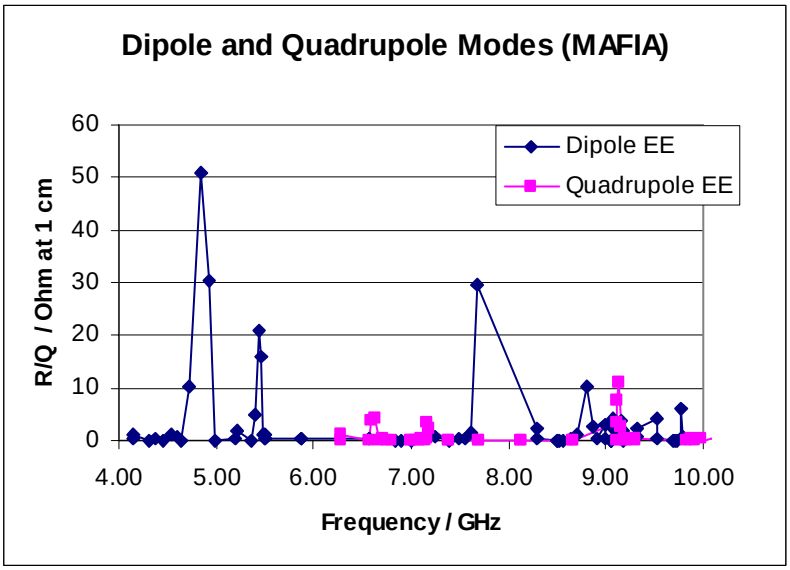

Figure 24: R/Q values of dipole and quadrupole modes (EE boundary conditions, MAFIA calculation) at an radial offset of 1 cm.

The frequencies of the quadrupole modes from the first and second passband are below the cutoff frequency of the beam pipe, which is 7.2864 GHz for TE Quadrupole modes. The mode with the highest R/Q value below the cutoff frequency of the beam pipe is show in Figure 25.
The mode with highest R/Q value in the considered frequency range up to 10 GHz is the mode #30 with R/Q = 11.1 Ohm at 1 cm radial offset. The electric field of this mode is shown in Figure 26. There is a small electric field component in the beam pipe, which is shown in Figure 27.

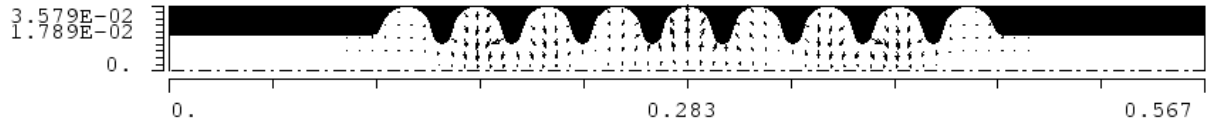

Figure 25: Electric field of the quadrupole mode #5, f=6.62 GHz, R/Q = 4.3 Ohm/cm^4 (EE boundary condition, MAFIA calculation)

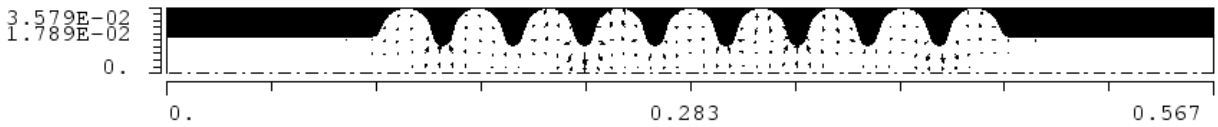

Figure 26: Electric field of the quadrupole mode #30, f=9.13 GHz, R/Q = 11.1 Ohm/cm^4 (EE boundary condition, MAFIA calculation).

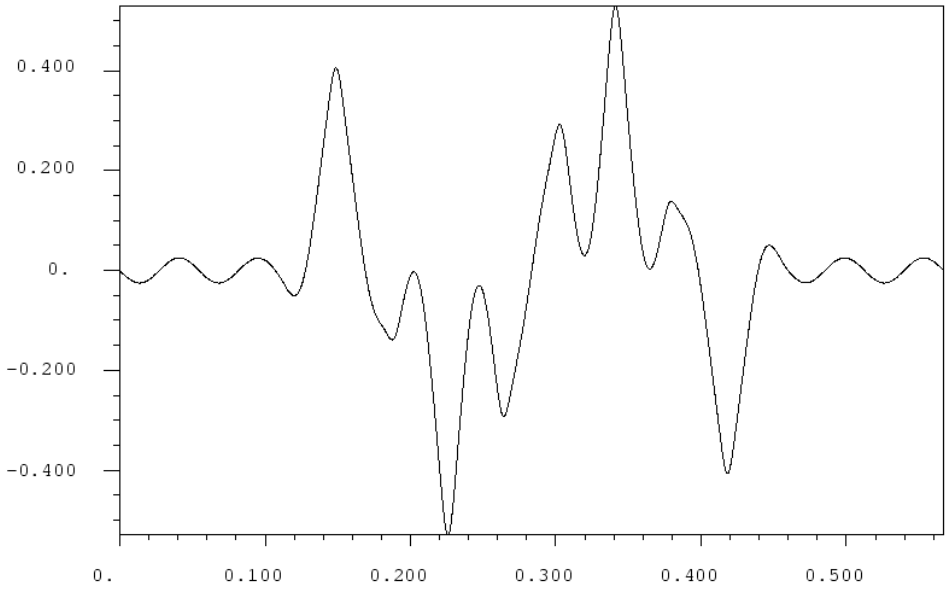

Figure 27: Radial field component of the electric field versus z of the quadrupole mode #30, f=9.13 GHz, (EE boundary condition, MAFIA calculation). The field component E_r (r,z) is plotted at the radial position r= 1 cm.

The External Q-values of Monopole, Dipole and Quadrupole Modes

The HFFS code has been used to model the 9-cell cavity together with the main input couplers and two HOM couplers. The cavity and the couplers are shown in Figure 28. A more detailed view of the HOM couplers and their location with respect to the end cells is shown in Figure 29. Small current density probes have been put into each cavity to excite the modes of the cavity. The phases of the current densities are related to each other in way a beam would excite the modes: $\Delta\phi = 2\pi\ f\ \ g/c$ (phase difference of the current density from cell to cell), g is the length of one cavity cell and f the excitation frequency. The current densities have been placed 2 mm off axis in the x and y direction of each cell to excite the dipole modes in both polarization directions. The x-axis is defined as the axis of the main input coupler. The response due to the excitation has been monitored at the coupler ports.

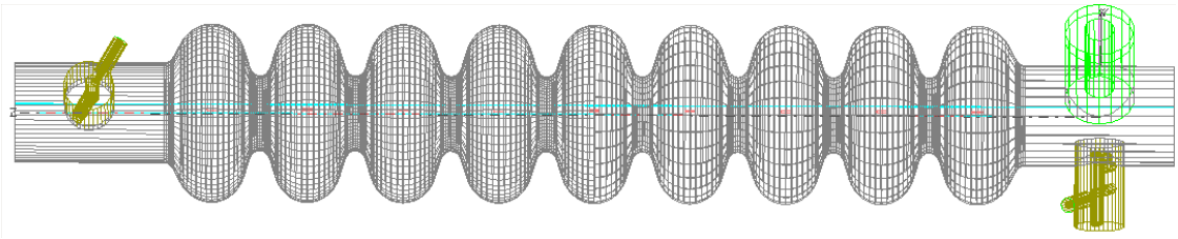

Figure 28: Three dimensional model (HFFS) of the 9-cell cavity with input and HOM couplers.

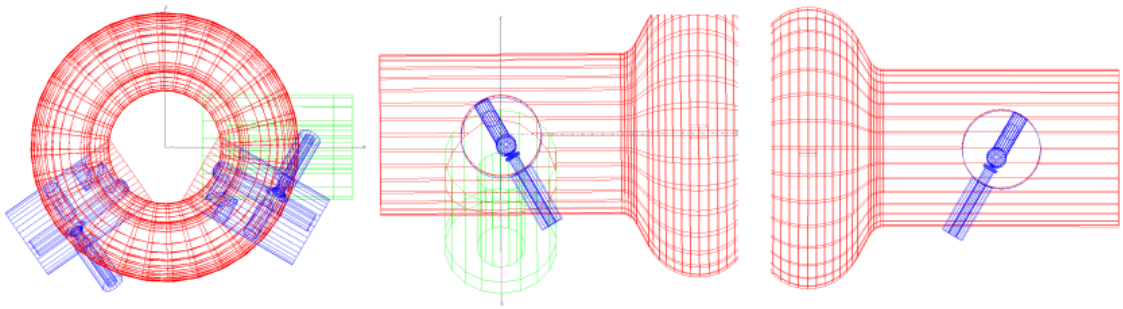

Figure 29: Detailed view of the HOM couplers (modeled with HFFS). The location of the HOM antennae with respect to the cavity end cells are shown as well as the azimuthal orientation of the couplers with respect to each other.

The response to the current density excitation at the HOM coupler port as a function of the excitation frequency is shown in Figure 30 for electric and in Figure 31 for magnetic boundary conditions at both ends of the cavity. The red line corresponds to an offset of the excitation current density in the x-direction, and the green line to an offset in the y-direction.

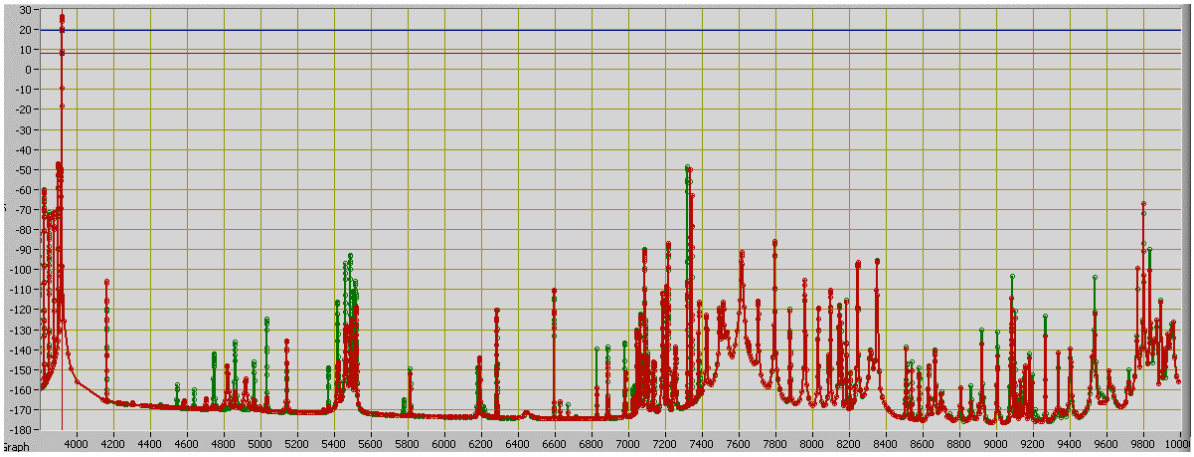

Figure 30: Response (dB) to the current density excitation (S_{12} parameter) at the HOM coupler port versus frequency (MHz) up to a frequency of 10GHz. Electric boundary conditions are used at both ends of the cavity. The red line corresponds to an offset of the excitation current density in the x-direction of 2 mm, and the green line to an offset in the y-direction of 2 mm.

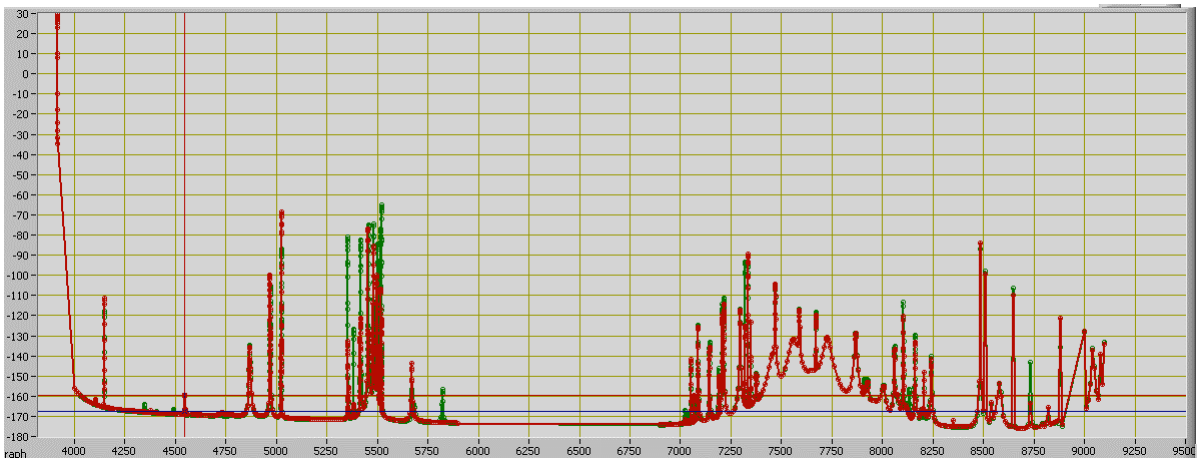

Figure 31: Response (dB) to the current density excitation (S_{12} parameter) at the HOM coupler port versus frequency (MHz) up to a frequency of about 9 GHz. Magnetic boundary conditions are used at both ends of the cavity. The red line corresponds to an offset of the excitation current density in the x-direction of 2 mm, and the green line to an offset in the y-direction of 2 mm.

An analysis of the HFFS results gives an external Q-value of about $1 \cdot 10^6$ for the accelerating mode. A list of the external Q-values of the monopole modes from the first passband is given in Table 3. The results for the dipole modes are presented in Table 4 and Table 5. The results for quadrupole modes are listed in Table 6. The modes are listed with respect to their frequency. A frequency which is printed in bold face indicates a mode with a phase velocity close to the speed of light. These modes are the most important for beam dynamics simulations. There are two table columns for the Q-values corresponding to the boundary conditions at the end of the cavity (EE: electric short at both ends, MM: magnetic short at both ends) used in the HFFS calculation in which the mode was found. The electric field of the first dipole mode from Table 4 is show in Figure 32.

Boundary:	EE
f /MHz	Q
3762.7	1.44E+07
3776.2	3.95E+06
3797	1.16E+07
3822.7	1.07E+06
3850.3	7.18E+05
3876.5	5.73E+05
3898	4.56E+05
3912.1	4.60E+05
3917.5	9.94E+05

Table 3: External Q-values of monopole modes from the first passband (calculated from HFFS results). Electric boundary conditions have been used at the end of the cavity.

Boundary:	EE	MM		EE	MM
f/ MHz	Q	Q	f/ MHz	Q	Q
4146.2		3.86E+05	5386.0		5.00E+02
4160.9	5.51E+05		**5414.3**		3.63E+03
4301.4	2.00E+03		**5417.6**		5.26E+04
4347.4		1.50E+03	**5418.1**	6.37E+03	
4544.5	1.86E+03		**5421.5**	1.02E+03	
4546.2		1.24E+03	**5451.6**		2.37E+04
4582.0	7.40E+02		**5455.6**		3.58E+04
4637.0	1.64E+03		**5459.9**	9.35E+03	
4701.5	8.50E+02		**5463.0**	1.10E+03	
4730.0		2.00E+02	5479.7		1.76E+04
4744.9	2.27E+03		5483.4		3.72E+04
4817.4	5.55E+02		5487.8	1.26E+04	
4860.3	1.46E+03		5490.0	1.80E+03	
4866.0		1.63E+03	5498.3		1.66E+04
4917.5	3.86E+02		5501.2		4.73E+04
4962.0	1.18E+03		5504.8	1.65E+04	
4968.6		1.61E+04	5506.7	2.50E+03	
4969.6		1.19E+04	5509.7		2.25E+04
4996.0	4.00E+02		5511.8		8.00E+04
5023.4		2.56E+04	5514.2	2.43E+04	
5024.2		8.43E+04	5515.7	4.10E+03	
5031.7	6.51E+03		5516.1		3.91E+04
5340.0	1.00E+03		5517.4		2.12E+05
5354.4		2.45E+05	5518.8	4.33E+04	
5357.3		1.85E+03	5519.2		1.50E+05
5366.4	6.22E+03		5519.8		6.09E+05
5369.5	8.00E+02		5520.1	1.59E+04	
5381.0		4.08E+04	5521.0	6.19E+03	

Table 4: External Q-values of dipole modes (calculated from HFFS results) up-to a frequency of about 6 GHz. Electric and magnetic boundary conditions have been used at the end of the cavity.

Boundary:	EE	MM		EE	MM
f/ MHz	Q	Q	f/ MHz	Q	Q
6826.1	9.49E+04		8639.0	<1000	
6826.8	7.04E+04		8649.4		2.94E+05
6849.9		8.20E+02	8650.0		3.25E+05
6885.1	2.39E+04		8730.8		4.81E+04
6887.2	1.29E+04		**8731.7**		3.64E+04
6978.6	1.08E+04		**8816.2**		6.22E+04
6982.0	4.37E+03		8817.2		1.90E+04
6949.0		7.00E+02	8879.8		3.42E+04
6978.6	1.08E+04		8931.8		1.90E+05
6982.0	4.37E+03		8932.1		1.42E+07
7072.0		8.20E+02	9075.6		1.06E+07
7334.7	5.00E+03		9075.6	7.08E+05	
7336.5		4.00E+03	9076.1		3.87E+06
7470.4		5.79E+03	9076.1	2.95E+05	
7588.2		2.86E+03	9076.3		1.75E+08
7670.3		1.19E+04	9076.8		3.53E+06
8507.2	1.44E+04		**9077.8**		8.38E+06
8509.2		1.66E+06	**9078.7**		2.11E+06
8510.0		3.53E+05	**9079.5**		**5.90E+06**
8511.5	9.75E+03		9079.6	2.95E+05	
8514.3		1.14E+06	9083.7		7.58E+05
8538.3	1.69E+04		9083.9	4.40E+04	
8541.2		8.54E+05	9085.1		1.54E+06
8542.1		1.67E+05	9085.3	1.46E+05	
8578.0		<1000	9098.9		1.70E+05
8579.5	6.03E+03		9100.6		1.88E+05
8586.8		9.73E+03	9100.9	8.59E+04	
8630.5	2.27E+03				

Table 5: External Q-values of dipole modes (calculated from HFFS results) in the frequency range between 6 GHz and 10 GHz. Electric and magnetic boundary conditions have been used at the end of the cavity.

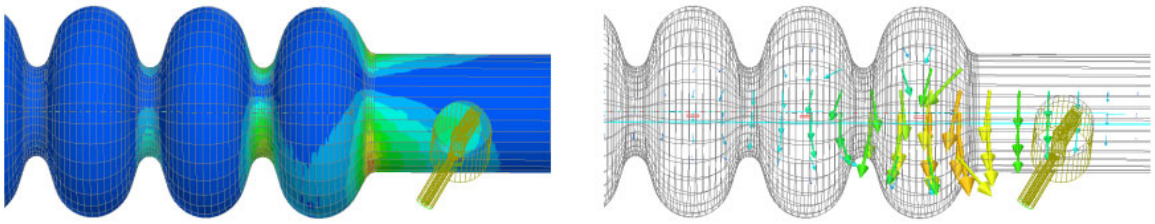

Figure 32: Electric field of the dipole mode f = 4.1462 GHz, R/Q=0.4 Ohm/cm^2, Qext=5.5 10^5 (HFFS calculation).

Boundary:	EE	MM		EE	MM
f/ MHz	Q	Q	f/ MHz	Q	Q
6281.4		6.78E+04	6807.1		5.62E+05
6281.5	1.16E+05		6807.1	1.99E+05	
6282.8		2.00E+04			
6284.2	1.05E+05		7022.2		3.00E+03
6573.9		1.70E+06	7022.4	4.08E+03	
6574.0		1.55E+06	7022.5		3.00E+03
6574.0	1.41E+06		7029.7		2.00E+03
6594.6		4.35E+05	7030.3	2.64E+03	
6594.6	3.07E+05		7029.9		2.00E+03
6594.6		3.43E+05	7067.0		7.53E+03
6594.6	4.00E+05		7067.1	6.00E+03	
6627.2	2.22E+05		7067.1		6.00E+03
6627.2		2.15E+05	7103.5		5.00E+03
6627.3		1.84E+05	7104.7	8.09E+03	
6627.4	1.72E+05		7104.1		5.00E+03
6669.2	1.20E+05		7138.1		6.63E+03
6669.2		6.51E+04	7138.6	6.26E+03	
6669.3	1.41E+05		7144.1		6.43E+03
6717.1		1.42E+05	**7167.0**		7.43E+03
6717.1	1.02E+05		**7167.5**	1.33E+04	
6717.2	1.04E+05		**7194.4**	2.19E+04	
6717.2		1.96E+05	7205.2		3.00E+04
6765.8	1.20E+05		7205.5		2.61E+04
6765.9		1.58E+05	7205.6	4.00E+04	
6765.9	1.20E+05		7215.1		3.20E+04
6790.5		5.71E+02	7215.3	1.82E+05	
6807.0	2.01E+05		7215.3		1.20E+04
6807.0		3.65E+05			

Table 6: External Q-values of quadrupole modes (calculated from HFFS results) up-to a frequency of about 7.7 GHz. Electric and magnetic boundary conditions have been used at the end of the cavity.

The external Q-value for almost all dipole modes in the considered frequency range which are synchronous with the beam (frequency printed in bold face) is smaller than$1 \cdot 10^5$. The exceptions are some modes in the 5th dipole passband (9 GHz) which have Q-values above $1 \cdot 10^6$. These modes are almost trapped in the cavity like the mode shown in Figure 21. The R/Q of these modes are about 4 Ohm/cm^2 and are therefore of some concern. There are more modes with a relatively high Q-value, like the mode shown in Figure 32 which has an external Q-value of about $5 \cdot 10^5$. Fortunately the R/Q of this mode is low (< 0.5 Ohm/cm^2). All dipole modes from the first and second dipole passband with high R/Q values are well damped with external Q-values well below $5 \cdot 10^4$.
The quadrupole modes are only important if the beam transverses the cavity with a large offset (say 1cm) with respect to the axis of the cavity. All Quadrupole modes with a larger R/Q-value have Q-values below $5 \cdot 10^5$, and seem to be sufficiently damped.

Conclusion

The higher order modes of a third harmonic (3.9 GHz) cavity with an increased end-cup iris have been investigated. The computer codes HFFS and MAFIA have been used to calculate the rf-parameters of the accelerating mode and higher order monopole, dipole and quadrupole modes up to a frequency of about 10 GHz. The obtained data are the basis for beam dynamics simulations of the TESLA test facility photoinjector.
The frequency of almost all dipole modes is above the cutoff frequency of the beam pipe. The R/Q value of these modes depends therefore on the boundary conditions at the end of the cavity. Electric and magnetic boundary conditions have been considered in this report. There are a few quasi trapped modes with almost no electric field in the beam pipe and in the cavity end cells at frequencies of about 9 GHz. The external Q values of the monopole, dipole and quadrupole modes have been studied using the HFFS code which was applied to a three dimensional cavity model with a main input coupler and two HOM couplers. Most external Q values of the dipole modes in the considered frequency range of up to 10 GHz are below $1 \cdot 10^5$. First beam dynamics simulations [5] indicate that Q values of $1 \cdot 10^5$ are tolerable. The modes with larger external Q values have mostly small R/Q values. The modes of the 5^{th} dipole passband are of some concern since there exist a few modes with Q values of about $6 \cdot 10^7$ which are nearly trapped in the cavity. These modes should be considered in further beam dynamics simulations.

Appendix A: Monopole Modes

The results from a MAFIA calculation with electric boundary conditions are summarized in the following table.

mode #	f/GHz	(R/Q)/ Ohm	G1/Ohm
1	3.7455	0.007	255.3
2	3.7589	0.060	256.2
3	3.7796	0.085	257.5
4	3.8051	0.166	259.3
5	3.8325	0.278	261.2
6	3.8585	0.194	263.1
7	3.8799	0.317	264.7
8	3.8940	0.134	265.6
9	3.8991	374.748	261.8
10	5.7689	19.558	388.9
11	5.7689	1.257	388.9
12	6.0129	3.373	408.0
13	6.0129	12.026	408.0
14	6.4409	18.560	442.8
15	6.4409	3.243	442.8
16	6.9339	16.700	467.7
17	6.9339	4.694	467.8
18	7.0410	0.225	435.2
19	7.0790	1.586	436.9
20	7.1349	0.123	439.2
21	7.2036	4.334	443.0
22	7.2799	1.204	449.5
23	7.3585	3.594	459.5
24	7.4344	15.939	471.1
25	7.5054	23.219	475.5
26	7.5765	42.874	438.8
27	7.6398	2.134	546.1
28	7.7180	18.580	503.4
29	7.7964	0.621	507.9
30	7.8737	0.876	522.8
31	7.9477	0.576	544.3
32	8.0163	0.019	570.7
33	8.0768	0.021	600.8
34	8.1255	0.040	631.9
35	8.1578	0.005	657.8
36	8.3334	1.943	590.7
37	8.3334	3.885	590.7
38	9.1175	7.103	615.8
39	9.1175	0.914	615.8
40	9.7897	0.001	565.0

Appendix B: Dipole Modes

The results from a MAFIA calculation with electric (EE) and Magnetic (MM) boundary conditions are summarized in the following table.

MAFIA	EE			MM		
mode #	f/GHz	R/Q / Ohm/cm^2	G1/Ohm	f/GHz	R/Q / Ohm/cm^2	G1/Ohm
1	4.1505	0.23	259.8	4.1499	0.24	259.3
2	4.1507	1.31	260.0	4.1500	1.30	259.5
3	4.3019	0.00	235.3	4.3017	0.00	235.2
4	4.3641	0.29	243.2	4.3626	0.26	242.6
5	4.4514	0.00	251.5	4.4316	0.08	248.5
6	4.5428	1.07	258.5	4.4511	0.00	254.2
7	4.5993	0.82	269.9	4.4784	0.31	259.8
8	4.6422	0.13	280.4	4.5729	1.22	264.6
9	4.7260	10.39	281.2	4.6826	1.56	269.9
10	4.8341	50.70	277.3	4.7764	26.92	277.9
11	4.9282	30.41	269.0	4.8464	32.04	293.5
12	4.9909	0.00	258.7	4.9173	22.44	302.1
13	5.2008	0.31	373.1	4.9955	7.53	296.8
14	5.2034	2.09	364.9	5.0248	3.83	269.6
15	5.3588	0.04	510.7	5.3525	0.06	529.0
16	5.4052	4.99	454.2	5.3925	2.06	470.7
17	5.4427	20.91	426.2	5.4271	10.69	438.4
18	5.4676	16.01	410.4	5.4526	17.11	419.1
19	5.4826	0.96	400.8	5.4709	9.54	406.0
20	5.4908	1.25	394.9	5.4833	0.44	397.0
21	5.4946	0.31	392.1	5.4906	0.34	391.2
22	5.4955	0.47	389.4	5.4942	0.03	388.1
23	5.8635	0.39	463.5	5.5518	3.17	417.4
24	5.8635	0.40	463.5	5.5518	2.69	417.4
25	6.5607	0.34	585.6	6.2125	0.38	564.1
26	6.5609	0.39	585.6	6.2125	0.87	564.1
27	6.8264	0.01	612.8	6.7998	0.07	626.7
28	6.9027	0.04	613.5	6.8271	0.07	646.3
29	7.0050	0.06	614.2	6.8938	0.13	652.0
30	7.1248	0.19	613.4	6.9909	0.13	649.9
31	7.2563	0.57	607.5	7.1017	0.11	637.4
32	7.3853	0.01	598.1	7.2166	0.02	614.3
33	7.4907	0.47	590.8	7.3373	0.85	584.0
34	7.5636	0.26	565.9	7.4621	0.53	547.4
35	7.6206	1.37	513.7	7.5762	2.89	507.0
36	7.6685	29.53	470.7	7.6581	24.46	471.8
37	8.3027	2.38	731.1	7.9054	1.98	743.6
38	8.3027	0.50	731.1	7.9054	3.17	742.9
39	8.4912	0.11	469.5	8.4888	0.34	470.5
40	8.4968	0.09	485.2	8.4930	0.02	482.7

MAFIA	EE			MM		
mode #	f/GHz	R/Q / Ohm/cm^2	G1/Ohm	f/GHz	R/Q / Ohm/cm^2	G1/Ohm
41	8.5240	0.15	488.9	8.5205	0.38	481.8
42	8.5690	0.11	514.1	8.5630	0.02	506.0
43	8.6336	0.40	555.8	8.6208	1.41	548.7
44	8.7158	1.03	617.0	8.6811	0.05	643.1
45	8.8001	10.35	701.1	8.7251	4.72	798.3
46	8.8630	2.59	813.1	8.7702	1.76	865.8
47	8.9185	0.27	893.3	8.8290	5.74	853.2
48	8.9857	3.19	999.9	8.8715	1.95	879.3
49	8.9967	0.24	904.4	8.9185	0.27	894.3
50	9.0594	0.00	1093.6	8.9903	3.56	1009.8
51	9.0602	0.05	1093.4	9.0001	0.32	920.0
52	9.0618	0.06	1096.7	9.0594	0.00	1093.6
53	9.0653	2.19	1112.8	9.0602	0.05	1093.5
54	9.0736	4.06	1174.2	9.0619	0.08	1097.1
55	9.0961	0.56	1376.1	9.0655	2.36	1114.5
56	9.1613	1.77	637.9	9.0741	3.95	1182.2
57	9.1615	3.98	632.9	9.0976	0.37	1410.2
58	9.1766	0.04	975.7	9.2239	0.17	718.5
59	9.1782	1.81	1000.7	9.2240	0.08	718.8
60	9.3200	0.67	627.8	9.4253	0.11	736.2
61	9.3201	2.25	627.9	9.4258	0.03	736.4
62	9.5319	4.15	659.8	9.5827	0.32	1162.1
63	9.5325	0.26	660.1	9.5837	0.01	1166.4
64	9.6891	0.00	642.4	9.6371	0.48	716.7
65	9.7071	0.01	643.0	9.6376	0.84	717.0
66	9.7349	0.07	644.6	9.6909	0.01	645.0
67	9.7637	0.47	650.4	9.7115	0.03	646.7
68	9.7823	5.97	661.4	9.7425	0.35	647.4
69	9.7956	0.67	664.7	9.7783	1.16	648.4
70	9.8190	0.23	657.6	9.8138	0.35	650.3

The results from a HFFS calculation with electric (EE) and Magnetic (MM) boundary conditions are summarized in the following table.

HFSS	EE		MM	
mode #	f/ GHz	R/Q / Ohm/cm^2	f / GHz	(R/Q) / Ohm/cm^2
1	4.1442	0.42	4.1435	0.28
2	4.1444	1.12	4.1437	1.26
3	4.2923	0.00	4.2917	0.00
4	4.3551	0.29	4.3535	0.26
5	4.4433	0.00	4.4261	0.07
6	4.5365	1.08	4.4481	0.00
7	4.5954	0.79	4.4728	0.33
8	4.6381	0.16	4.5657	1.21
9	4.7206	10.27	4.6762	1.52
10	4.8291	49.85	4.7714	26.79
11	4.9239	30.49	4.8424	31.99
12	4.9872	0.00	4.9136	21.79
13	5.1989	0.29	4.9924	7.45
14	5.2016	2.05	5.0217	3.78
15	5.3567	0.04	5.3499	0.05
16	5.4043	5.06	5.3909	2.06
17	5.4426	20.90	5.4262	10.48
18	5.4680	15.95	5.4523	16.94
19	5.4834	0.98	5.4711	9.72
20	5.4916	1.27	5.4839	0.49
21	5.4957	0.31	5.4864	0.56
22	5.4966	0.47	5.4942	0.33
23	5.8622	1.26	5.4981	0.04
24	5.8622	1.03	5.5529	3.03
25	6.5582	0.33	5.5529	3.04
26	6.5584	0.39	6.2108	0.40
27	6.8198	0.00	6.2108	0.82
28	6.8968	0.04	6.7891	0.06
29	6.9997	0.06	6.8186	0.06
30	7.1200	0.19	6.8860	0.15
31	7.2526	0.56	6.9836	0.13
32	7.3826	0.02	7.0951	0.11
33	7.4890	0.48	7.2109	0.02
34	7.5626	0.25	7.3327	0.78
35	7.6201	1.31	7.4593	0.50
36	7.6686	28.87	7.5760	2.71
37	7.9165	0.00	7.6604	23.32
38	7.9167	0.00	7.9059	2.06
39	8.1827	0.03	7.9060	3.11
40	8.1874	0.01	7.9156	0.00

HFSS	EE		MM	
mode #	f/ GHz	R/Q / Ohm/cm^2	f / GHz	(R/Q) / Ohm/cm^2
41	8.1945	0.00	7.9157	0.00
42	8.2032	0.00	8.1826	0.03
43	8.2120	0.00	8.1873	0.01
44	8.2197	0.00	8.1945	0.00
45	8.2249	0.00	8.2031	0.00
46	8.3023	1.57	8.2119	0.00
47	8.3024	1.54	8.2196	0.00
48	8.4930	0.11	8.2248	0.00
49	8.4983	0.08	8.4908	0.35
50	8.5257	0.16	8.4948	0.01
51	8.5703	0.11	8.5224	0.36
52	8.6345	0.41	8.5646	0.02
53	8.7155	1.03	8.6219	1.44
54	8.7560	0.00	8.6812	0.04
55	8.7560	0.00	8.7240	4.57
56	8.7982	10.22	8.7556	0.00
57	8.7992	0.01	8.7558	0.00
58	8.8060	0.00	8.7683	1.67
59	8.8161	0.00	8.7990	0.00
60	8.8268	0.00	8.8058	0.00
61	8.8369	0.00	8.8154	0.00
62	8.8449	0.00	8.8266	5.67
63	8.8611	2.57	8.8266	0.14
64	8.9154	0.35	8.8366	0.00
65	8.9811	3.30	8.8447	0.00
66	8.9932	0.22	8.8499	0.00
67	9.0540	0.00	8.8683	1.98
68	9.0562	0.06	8.9153	0.34
69	9.0595	2.13	8.9853	3.71
70	9.0674	4.05	8.9963	0.28
71	9.0891	0.57	9.0541	0.00
72			9.0547	0.05
73			9.0563	0.08
74			9.0677	3.96
75			9.0903	0.39
76			9.2155	0.19
77			9.2160	0.16

Appendix C: Quadrupole Modes

The results from a MAFIA calculation with electric (EE) and Magnetic (MM) boundary conditions are summarized in the following table.

MAFIA	EE			MM		
mode #	f/ GHz	R/Q / Ohm/cm^4	G1 / Ohm	f/GHz	(R/Q) / Ohm/cm^4	G1/ Ohm
1	6.2719	0.04	413.3	6.2719	0.01	413.3
2	6.2719	1.19	413.3	6.2719	1.23	413.3
3	6.5694	0.19	398.9	6.5694	0.19	398.9
4	6.5895	3.78	404.3	6.5895	3.78	404.3
5	6.6221	4.34	412.6	6.6221	4.34	412.6
6	6.6627	0.16	424.0	6.6627	0.16	424.0
7	6.7093	0.30	439.9	6.7093	0.30	439.9
8	6.7574	0.00	463.0	6.7574	0.00	463.0
9	6.7995	0.04	496.6	6.7995	0.04	496.6
10	6.9970	0.13	376.5	6.9970	0.13	376.5
11	7.0056	0.08	388.8	7.0056	0.08	388.8
12	7.0420	0.15	407.6	7.0420	0.15	407.6
13	7.0773	0.00	426.4	7.0773	0.00	426.3
14	7.1106	0.25	440.7	7.1106	0.25	440.7
15	7.1377	0.10	452.6	7.1377	0.10	452.6
16	7.1593	0.57	461.3	7.1593	0.57	461.3
17	7.1740	3.51	468.2	7.1740	3.51	468.2
18	7.1835	2.14	471.6	7.1835	2.14	471.6
19	7.3995	0.00	343.0	7.3156	0.00	332.9
20	7.3995	0.04	343.0	7.3156	0.02	332.9
21	7.7019	0.04	378.4	7.5309	0.02	360.7
22	7.7019	0.02	378.4	7.5309	0.04	360.7
23	8.1356	0.07	427.4	7.9054	0.07	407.6
24	8.1356	0.07	427.4	7.9054	0.05	407.6
25	8.6663	0.08	482.2	8.3894	0.16	465.4
26	8.6663	0.13	482.2	8.3894	0.13	465.4
27	9.1106	3.26	389.3	8.9657	0.13	532.4
28	9.1115	0.16	396.0	8.9657	0.18	532.4
29	9.1198	7.70	391.1	9.1120	2.02	383.1
30	9.1323	11.11	403.1	9.1135	0.29	390.3
31	9.1513	2.80	420.1	9.1208	8.96	391.9
32	9.1738	0.03	443.2	9.1330	11.19	402.9
33	9.1960	0.22	469.9	9.1519	2.54	419.4
34	9.2131	0.00	491.8	9.1741	0.06	442.3
35	9.2926	0.13	527.1	9.1962	0.23	469.1
36	9.2926	0.22	527.1	9.2132	0.00	491.5
37	9.8398	0.00	484.3	9.6303	0.27	584.1
38	9.8722	0.28	506.9	9.6303	0.05	584.2
39	9.9257	0.01	538.2	9.8430	0.00	486.4
40	9.9743	0.56	577.2	9.8832	0.11	514.3

MAFIA	EE			MM		
mode #	f/ GHz	R/Q / Ohm/cm^4	G1 / Ohm	f/GHz	(R/Q) / Ohm/cm^4	G1/ Ohm
41	10.0131	0.19	606.6	9.9532	0.13	551.1
42	10.0798	0.47	631.0	10.0487	1.05	596.1
43	10.1840	0.07	671.8	10.1594	0.09	643.7
44	10.3006	0.04	730.0	10.2670	0.05	688.5
45	10.4083	0.02	809.3	10.3470	0.04	720.0
46	10.4842	0.04	910.8	10.4018	0.00	753.2
47	10.5358	0.05	971.7	10.4626	0.00	822.8
48	10.6239	0.01	1178.9	10.5129	0.04	945.9
49	10.6300	0.21	1180.8	10.5439	0.04	1003.1
50	10.6896	0.00	1146.0	10.6239	0.01	1178.6
51	10.6942	0.20	1217.8	10.6300	0.21	1179.0
52	10.6956	0.02	1247.1	10.6896	0.00	1146.3
53	10.6961	0.00	1274.3	10.6942	0.20	1217.9
54	10.6962	0.81	1276.3	10.6956	0.02	1247.1
55	10.6979	0.40	1273.9	10.6961	0.00	1274.3
56	10.7919	0.01	744.7	10.6962	0.81	1276.3
57	10.7919	0.03	744.6	10.6979	0.40	1273.9
58	11.3423	0.16	683.1	11.1617	0.00	795.5
59	11.3423	0.26	683.1	11.1617	0.06	795.5
60	11.4208	0.00	648.2	11.3523	0.21	706.7
61	11.4209	0.00	646.2	11.3523	0.24	706.6
62	11.4248	0.00	650.9	11.4213	0.00	646.1
63	11.4252	0.03	646.5	11.4219	0.00	646.7
64	11.4320	0.02	644.0	11.4282	0.00	650.8
65	11.4381	0.17	643.1	11.4284	0.01	649.6

Acknowledgment

We would like to thank Michaela Marx for her help with the MAFIA calculations and Leo Bellantoni for carefully reading the manuscript. One of the authors (R.W.) would like to thank Helen Edwards and Leo Bellantoni for their kind hospitality during his visit to FERMILAB in 2002 (Nov. 20 to Dec. 11).

References

[1]

K. Flöttmann, T. Limberg, Ph. Piot,
Generation of ultrashort electron bunches by cancellation of nonlinear distortions in the longitudinal phase space,
TESLA-FEL-2001-06

[2]

W.F.O. Müller, J. Sekutowicz, R. Wanzenberg, T. Weiland,
A Design of a 3rd Harmonic Cavity for the TTF 2 Photoinjector
TESLA-FEL 2002-05, July 2002

[3]

HFFS, 3D EM Simulation Software for RF Design,
Ansoft Corporate Headquarters, Four Station Square, Pittsburgh, PA 15219-1119, USA

[4]

MAFIA Release 4,
CST GmbH, Bad Nauheimer Str. 19, 64289 Darmstadt, Germany

[5]

P.Piot,
Private communication